ACS APPLIED MATERIALS & INTERFACES

Research Article

www.acsami.org

Dual-Responsive Polymer Coated Superparamagnetic Nanoparticle for Targeted Drug Delivery and Hyperthermia Treatment

Santanu Patra,[†] Ekta Roy,[†] Paramita Karfa,[†] Sunil Kumar,[†] Rashmi Madhuri,*[,†] and Prashant K. Sharma[‡]

[†]Department of Applied Chemistry, Indian School of Mines, Dhanbad, Jharkhand 826 004, India

[‡]Functional Nanomaterials Research Laboratory, Department of Applied Physics, Indian School of Mines, Dhanbad, Jharkhand 826 004, India

Supporting Information

ABSTRACT: In this work, we have prepared water-soluble superparamgnetic iron oxide nanoparticles (SPIONs) coated with a dual responsive polymer for targeted delivery of anticancer hydrophobic drug (curcumin) and hyperthermia treatment. Herein, superparamagnetic mixed spinel ($MnFe_2O_4$) was used as a core material (15−20 nm) and modified with carboxymethyl cellulose (water-soluble component), folic acid (tagging agent), and dual responsive polymer (poly-*N* isopropylacrylamide-*co*-poly glutamic acid) by microwave radiation. Lower critical solution temperature (LCST) of the thermoresponsive copolymer was observed to be around 40 °C, which is appropriate for drug delivery. The polymer-SPIONs show high drug loading capacity (89%) with efficient and fast drug release at the desired pH (5.5) and temperature (40 °C) conditions. Along with this, the SPIONs show a very fast increase in temperature (45 °C in 2 min) when interacting with an external magnetic field, which is an effective and appropriate temperature for the localized hyperthermia treatment of cancer cells. The cytocompatibility of the curcumin loaded SPIONs was studied by the methyl thiazol tetrazolium bromide (MTT) assay, and cells were imaged by fluorescence microscopy. To explore the targeting behavior of curcumin loaded SPIONs, a simple magnetic capturing system (simulating a blood vessel) was constructed and it was found that ∼99% of the nanoparticle accumulated around the magnet in 2 min by traveling a distance of 30 cm. Along with this, to explore an entirely different aspect of the responsive polymer, its antibacterial activity toward an *E. coli* strain was also studied. It was found that responsive polymer is not harmful for normal or cancer cells but shows a good antibacterial property.

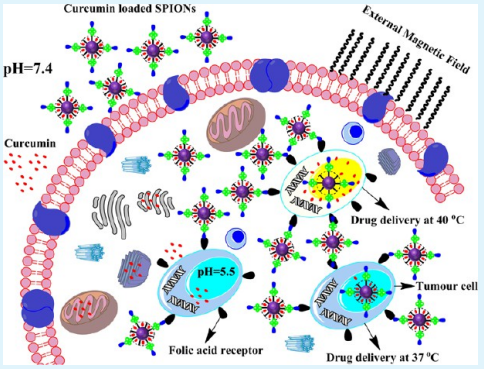

KEYWORDS: *targeted drug delivery, hyperthermia, curcumin, superparamagnetic nanoparticle, dual responsive polymer, cytotoxicity study, cell imaging*

1. INTRODUCTION

In the last few decades, nanotechnology has emerged as one of the very important fields of medicine and more specifically in targeted drug delivery. The therapeutic index of nearly all drugs currently being used would be improved if they were more efficiently delivered to their biological targets through appropriate application of nanotechnologies.[1] The best way to increase the efficacy and reduce the toxicity of any drug is to direct the drug to its target and maintain its concentration at the site for a sufficient time for therapeutic action to take effect. The concept of a "targeted" drug delivery system includes the coordinating behavior of three components, the targeting moiety, the carrier, and the therapeutic drug, and the potential of targeted drug delivery will be decided by proper functioning of all these three components.

In the recent years, several studies have been done and it was found that, having good carrier and targeting moieties, most of the currently available drugs have limited potential because they are very toxic and insoluble in water, possess side-effects, or are very expensive and thus beyond the reach of the majority. Curcumin is one of them, a polyphenol type compound derived from the rhizome or root of the plant *Curcuma longa*, a perennial herb belonging to the ginger family that is cultivated extensively in south and southeast tropical Asia (India, Japan). Research over the last few decades has shown that curcumin is a potent anti-inflammatory agent with strong therapeutic potential against a variety of cancers such as breast cancer, cervical cancer, pancreatic cancer, and many more.[2] Curcumin has been shown to suppress transformation, proliferation, and metastasis of tumors. It also inhibits proliferation of cancer cells by arresting them in various phases of the cell cycle and by inducing apoptosis.

Despite the excellent properties, it shows very limited application in cancer treatment because of its hydrophobic nature which shows low solubility, poor stability in aqueous solution (11.0 ng mL^{-1}), rapid degradation in physiological conditions, active binding with serum proteins, and fast clearance from circulation.[3] Along with this, the clinical trials

Received: February 27, 2015
Accepted: April 20, 2015
Published: April 20, 2015

DOI: 10.1021/acsami.5b01786
ACS Appl. Mater. Interfaces 2015, 7, 9235−9246

Scheme 1. Schematic Illustration of the Tumor Cell Uptake of Curcumin with and without Drug Carrier[a]

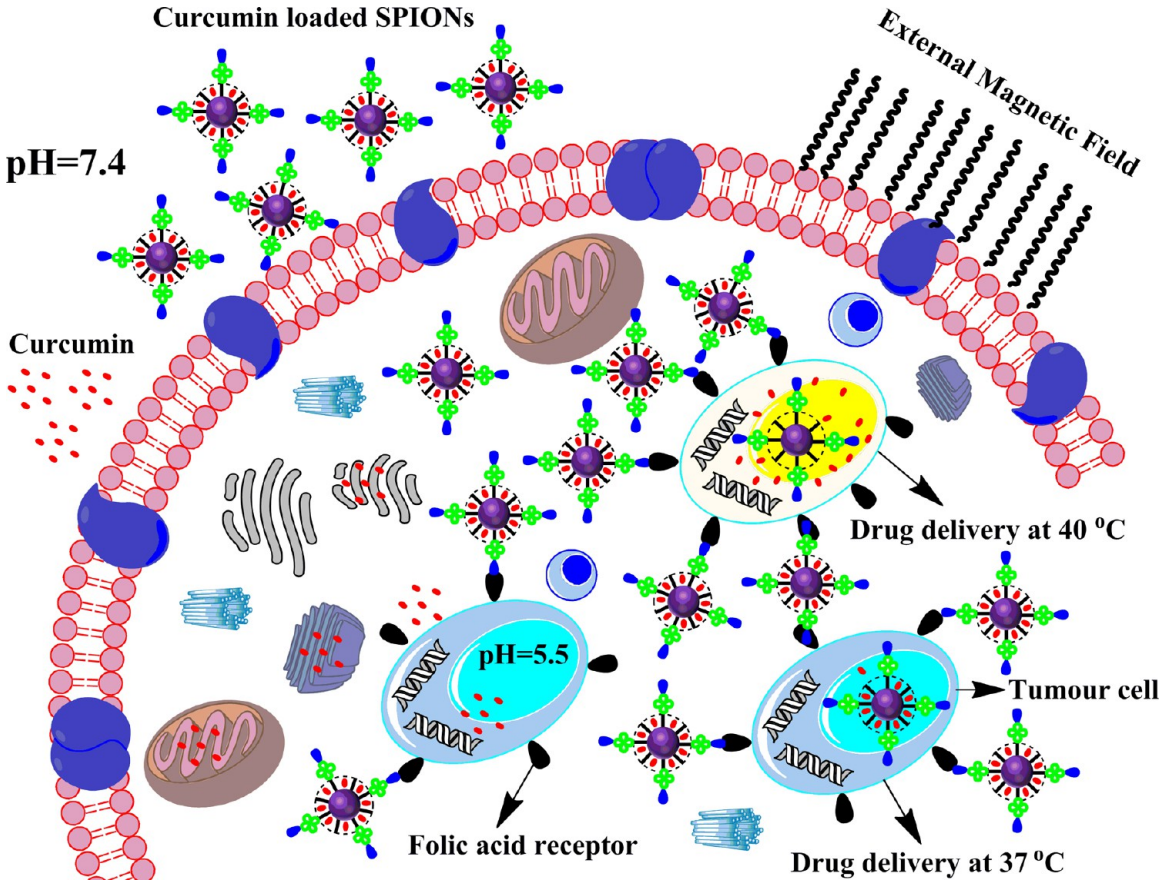

[a]Along with representation of their promoted and targeted uptake in the presence of external magnetic field.

also demonstrated the low or no therapeutic effect of free oral curcumin on various types of cancer. To address these problems and enhance solubility, stability, and the pharmacokinetic profile of curcumin, two different pathways of research have been adopted. One area is the modification of curcumin by making its conjugates with cyclodextrins,[4] cyclodextrin dimers,[5] poly(β-cyclodextrins),[6] alginate−cyclodextrin carriers,[7] only alginate,[8] or calix [4] arene structures.[9] The second route focuses on the development of new targeted drug delivery systems such as surfactant complexes,[10] liposomes,[11] liposome-based hybrid carriers,[12] hydrogels,[13] nanoemulsions,[14] nanosuspensions,[15] solid lipid nanoparticles,[16] polymeric and magnetic nanoparticles,[17] etc. Among them, magnetic targeting using superparamagnetic iron oxide nanoparticles (SPIONs) is the most popular way to achieve this goal. When the size of the magnetic nanoparticles (magnetite, Fe_3O_4, and spinel ferrites, $MeFe_2O_4$, where Me = Co, Mg, Mn, Zn)[18] decreases to below a critical size, (∼15−20 nm), each individual nanoparticle has a large constant magnetic moment and behaves like a giant paramagnetic atom with a fast response to applied magnetic fields with negligible remanence and coercivity.[19] These features make SPIONs attractive for a wide range of biomedical applications because the magnetization can be controlled by an external magnetic field without the risk of magnetic attraction at room temperature.[19] They can also be designed to generate heat when a high frequency magnetic field is applied for hyperthermia treatment where cancer cells usually get ablated at around 42−45 °C and other healthy body cells remain safe.[20]

A single problem associated with the use of SPIONs in drug delivery is their high surface to volume ratio, as they tend to agglomerate forming clusters in the bloodstream. Plasma proteins adsorb on the nanoparticles surface and macrophage cells activate the clearance mechanism (opsonization), before they reach the target site. An effective way of cellular internalization is to modify the surface of SPIONs with a ligand or some hydrophilic and biocompatible polymer that can be efficiently taken up by the cancer cells. To address and overcome these problems, several modifications of SPIONs or magnetic nanoparticles (MNPs) have been reported so far, viz., modification with polyethylene glycol-polylactic acid block copolymer,[21] 3-aminopropyltriethoxysilane,[22] chitosan, or oleic acid as shell[23] and PEG.[24]

Recently, stimuli responsive polymer (SRP) coated MNPs or SPIONs have become very popular in the field of targeted delivery and cancer therapy. Responsive polymers possess an interesting property; i.e., they can undergo structural and physical transitions (like phase, solubility, hydrophobicity, conformation, etc.) with change in the environmental conditions (i.e., change in pH, ionic strength, light, temperature, magnetic or electric properties, etc.).[25] Among the previously reported SRPs, temperature and pH-responsive polymers are more popular, where the drug release depends upon change in the temperature and pH values varies in different tissues and cellular compartments (the extracellular environment of a tumor has a lower pH (∼5−6) than blood and normal tissues (pH 7.4).[26] One of the unique and exciting properties of the temperature-responsive polymers is the

DOI: 10.1021/acsami.5b01786
ACS Appl. Mater. Interfaces 2015, 7, 9235−9246

presence of a critical solution temperature (CST). Below this, the responsive polymer is soluble in water and, after heating, becomes insoluble, i.e., formation of emulsion.[27] Poly(*N*-isopropylacrylamide) (PNIPAm) is the widely used temperature-responsive polymer, and it exhibits a lower critical solution temperature (LCST) of around 32 °C, which is slightly lower than body temperature and not well suited for drug delivery. Several works have been reported to raise the LCST of polymer by addition of acrylamide,[28] acrylic acid,[29] styrene,[30] maleic acid,[31] 2-carboxy isopropylacrylamide,[32] *N*-hydroxymethyl acrylamide,[33] etc as comonomer. Similarly, various pH responsive drug delivery systems have been constructed for realizing the pH-triggered drug release. Nevertheless, most of these systems are only responsive to a single pH variation, either in the tumor extracellular environment or in the intracellular endo/lysosomal condition. To overcome or resolve all these drawbacks, multistimuli responsive polymers were developed. Recently, Sahoo et al. have reported a temperature (LCST = 31 °C) and pH (5.0) dual responsive core−shell magnetic nanoparticle coated with smart polymer as an anticancer drug carrier for doxorubicin and cancer cell-specific targeting agent.[34] Yadavalli et al. have reported a dual responsive PNIPAm−chitosan targeted magnetic nanopolymer for targeted drug delivery of curcumin (LCST = 45 °C).[35] However, the dual responsive polymer modified-MNPs for targeted delivery of curcumin or any hydrophobic anticancer drug are still under development.

We report a dual responsive (pH and temperature) polymer modified SPION as an anticancer drug carrier and cancer cell-specific targeting agent. Herein, we have tried three different and fresh modifications during the preparation of responsive SPIONs. First, we have modified SPIONs with carboxymethyl celluloses (CMC), which are very important derivatives of cellulose; they have good solubility and high chemical stability and are toxicologically innocuous. As a result, the SPIONs conjugated with CMC are soluble in water, and they are also used to anchor folic acid (tagging agent) onto the nanoparticle surface. Second, we have used glutamic acid (GA) as comonomer of NIPAm to raise the LCST of responsive polymer; additionally, it also adds the pH-responsive behavior in the resulting block-polymer. Third, we have synthesized the responsive polymer modified SPIONs by the microwave synthesis method. The microwave heating process has a high temperature, enabling the reactions in the solution to occur in a relatively short time, and thus, they are completed faster than those under conventional thermal conditions. With the application of these three new synthetic steps, we have synthesized a dual responsive, target-specific, drug carrier for curcumin (Scheme 1). The drug delivery by the proposed carrier in the different pH values (5.5 and 7.4) and temperatures (25, 37, and 40 °C) has been successfully explored. To investigate the real phase application of the proposed modified SPIONs, a cell viability assay and cancer-cell imaging was also performed. The polymer-modified SPIONs generated a very fast increase in temperature (45 °C in 2 min) when exposed to an external magnetic field. Along with this, to examine an entirely different aspect of the responsive polymer, its antibacterial activity toward an *E. coli* strain was also studied. It was found that the responsive polymer is not harmful for normal or cancer cells but shows a good antibacterial property.

2. EXPERIMENTAL SECTION

2.1. Materials. *N*-Isopropylacrylamide (NIPAm) (>98%), *N*,*N*-methylene bis acrylamide (BIS) (99%), sodium lauryl sulfate (SLS) (>95%), ammonium peroxo disulfate (APS) (≥98%), glutamic acid (GA) (≥99%), acryloyl chloride (>97%), carboxy methyl cellulose (CMC) (>97%), 3-dicyclohexylcarbodiimide (DCC) (99%), folic acid (FA) (>98%), and curcumin (>97%) were purchased from Sigma-Aldrich (India) and TCI chemicals (Germany). Manganous sulfate ($MnSO_4$) (98%), ferric chloride ($FeCl_3$) (99%), citric acid (99.5%), sodium hydroxide (NaOH) (98%), *N*-hydroxysuccinimide (NHS) (98%), and solvents like dimethyl sulfoxide (DMSO) (99%) and ethanol (99.9%) were procured from Spectrochem Pvt. Ltd. (India) and Merck (India). The TEM grids were purchased from TAAB Laboratories Equipment Ltd., 3 Minerva House, Calleva Park, Aldermaston, Berks, RG7 8NA, UK, through Aaryans International, ED-11B Pitampura, Madhuban Chowk, New Delhi, 11088. All materials were reagent grade and used as received.

2.2. Synthesis of CMC−Curcumin Conjugates. For the synthesis of CMC−curcumin conjugate, 50 mg of CMC was added to a water/DMSO mixture (10 mL, 1:1 v/v) and stirred vigorously for 5 h resulting in the finely suspended CMC solution. Then, 4.0 mg of DCC was added, and the reaction mixture was stirred for 1 h at 20 °C for the activation of carboxylate groups present in CMC. To the activated CMC suspension, 50 mg of curcumin dissolved in 10.0 mL of DMSO was added under N_2 (g) atmosphere, and the mixture was stirred for about 7 h at 60 °C. The resultant solution was cooled to room temperature and dialyzed for 1 day against DMSO and 3 days against deionized water using a dialysis membrane of molecular weight cutoff of 3500 to remove the unreacted molecules. The pure CMC−curcumin conjugate was stored in the refrigerator for further use.

2.3. Synthesis of CMC-Folic Acid Conjugate (CMC-FA). Folic acid (0.45 g) was dissolved in 10 mL of DMSO and mixed with DCC (0.78 mg) and NHS (0.98 mg) by stirring for 2 h at room temperature. Separately, 5.0 mg of CMC was dissolved in distilled water and added dropwise to the above mixture with continuous stirring for overnight. After completion of the reaction, the product was washed and dried in a vacuum oven.

2.4. Preparation of Water-Soluble $MnFe_2O_4$ Nanoparticles. First, $MnFe_2O_4$ was prepared according to a previously reported procedure.[36] In brief, $MnSO_4$ (1 mmol, 0.169 g) and $FeCl_3$ (2 mmol, 0.324 g) were dissolved in a minimum amount of water, followed by addition of 50 mL of NaOH. The mixture was heated at 70 °C with continuous stirring for half an hour. The nanoparticles were magnetically separated by a commercial magnet (Neodymium rare earth magnet) and washed with distilled water (n = 6). For the preparation of water-soluble SPIONs, the as prepared nanoparticles were conjugated with CMC-FA conjugate using the same procedure reported in Section 2.2, for the preparation of the CMC−curcumin conjugate, and the pure FA-CMC-SPIONs conjugate was stored at room temperature for further use.

2.5. Preparation of Glutamic Acid Monomer (2-Acrylamidopentanedioic Acid). Herein, we have synthesized GA-derivative and used it as the comonomer for responsive polymer synthesis.[37,38] In brief, 10.0 mL of 0.5 M acryloyl chloride was added into the 0.5 M cool basic solution of GA (10.0 mL) and stirred for 1 h at 40 °C. After the completion of the reaction, the mixture was acidified with 37% HCl (pH = 2), extracted with ethyl acetate, and stored in a vacuum desiccator (yield = 87%). The compound was characterized on the basis of elemental analysis [calculated (%) for $C_8H_{11}NO_5$: C = 41.13, H = 5.18, N = 7.99; found (%): C = 41.0, H = 5.21, N = 8.03] and FT-IR (cm^{-1}): 3290 (υ−O−H, −COOH group), 1680 (υ-C═O), 1600 (υ-C═C), 1210 (υ−C−O−, −COOH group).

2.6. Conjugation of GA-Monomer and FA-CMC-SPIONs. To the 0.5 mg of modified FA-CMC-SPIONs aqueous solution, 50 mL of 20 g L^{-1} GA-monomer solution was added. The mixture was continuously stirred at 65 °C for 2 h and naturally cooled to room temperature. The precipitated FA-CMC-SPIONs-GA was separated from the solution using magnetic decantation with a permanent

DOI: 10.1021/acsami.5b01786
ACS Appl. Mater. Interfaces 2015, 7, 9235−9246

Scheme 2. Proposed Graphical Representation for the Design of Poly-SPIONs

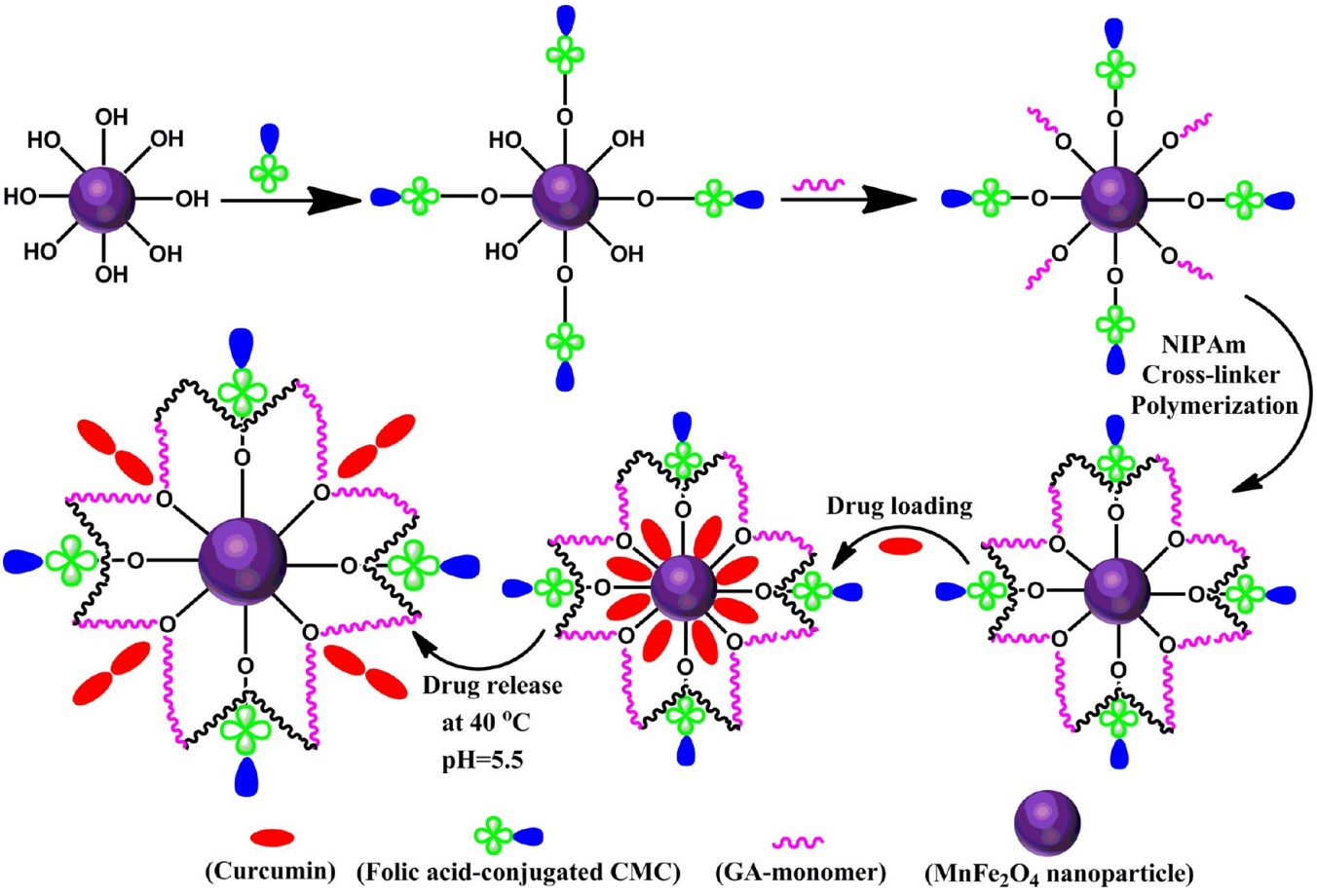

magnet, and modified nanoparticles were washed three times with deionized water and dried in a vacuum oven.

2.7. Synthesis of PNIPAm and PNIPAm-*co*-GA Modified SPIONs. In order to explore the utility of GA in the responsive polymer, two different polymers were synthesized: (1) with GA and (2) without GA as comonomer. In brief, the monomer (NIPAm 4.5 mmol), cross-linker (BIS, 0.225 mmol), the stabilizer (SLS 7 mg), and FA-CMC-SPIONs-GA (20 mg) were dissolved in 30.0 mL of distilled water, separately. Then, all of the components were mixed together, followed by addition of initiator (APS, 0.01 g dissolved in 4 mL of water). The mixture was degassed for 30 min in the presence of N_2 and kept in a domestic microwave for 40 min. After this, the prepared reponsive polymer (PNIPAm-*co*-GA) modified SPIONs (poly-SPIONs) were recovered by centrifugation at 10 000 rpm (9155*g*) and subjected to dialysis for 4 days. Similarly, PNIPAm modified SPIONs were also prepared as a reference without GA-monomer. The schematic representation of poly-SPIONs synthesis is shown in Scheme 2.

2.8. Physicochemical Characterization. Different intermediate conjugates and polymers were characterized by FT-IR spectra using a Varian Fourier Transform Infrared [FT-IR(USA)] spectrometer recorded in the range of 400−4000 cm^{-1} and discussed in the Supporting Information (Sections S1−S3 and Figures S1−S3). Particle sizes were measured using a dynamic light scattering (DLS) instrument (Zetasizer nano-S90, Malvern Instruments Ltd., UK) with a He−Ne laser beam at a wavelength of 633.8 nm. Measurements were made at 5 °C intervals using a temperature range of 25 to 45 °C. A delay time of 5 min was used at each temperature to ensure that the sample viscosity was equilibrated before the measurements were taken. Transmission electron microscopy (TEM; model Tecnai 30 G ^{2} S-Twin electron microscope) operated at 300 kV accelerating voltage and field emission scanning electron microscopy (FE-SEM; Zeiss Supra 55) were used to examine the morphology of the nanosystem. TEM samples were prepared by depositing 1.0 mL of the nanoparticle suspension on a copper TEM grid (200 mesh). The powder X-ray diffraction (XRD) study was carried out by a Bruker D8 Focus X-ray diffractometer instrument using a Cu target radiation source. Magnetization as a function of the field was recorded using a vibrating sample magnetometer (VSM; EG and G PAR 4500) by varying the field between −5 and +5 kOe. The temperature sensitive behavior, cloud point measurement, and optical density (O.D.) of the polymer modified SPIONs were evaluated with a UV−vis spectrophotometer (PerkinElmer Lambda 35, Singapore). The O.D. was measured over a temperature range of 25−46 °C. Confocal images were acquired using a Zeiss confocal laser scanning unit mounted on an LSM 710 fixed-stage upright microscope. Atomic force microscopy (AFM) was performed with a Bruker dimension icon nanoscope (Germany). For this, the sample was coated on a 1.0 × 1.0 cm glass plate and dried at room temperature.

2.9. In Vitro Drug Encapsulation Efficiency (EE) and Drug Loading (DL). To explore the maximum drug encapsulation and drug loading efficiency of poly-SPIONs, two parameters were optimized, i.e., amount of nanoparticle and concentration of drug. In this work, during drug loading, the CMC−curcumin conjugate was used in place of only curcumin. First, different amounts of nanoparticle (100, 110, 120, 130, and 150.0 μg) were taken and incubated with a constant amount of CMC−curcumin at 4 °C for 4 h. Second, a constant amount of nanoparticle was incubated with different concentrations of CMC−curcumin (1, 10, 100, and 1000 ppm). After loading, the nanoparticles were separated by an external magnet; the remaining curcumin present in the solution was extracted with 5.0 mL of ethyl acetate-propane-2-ol solution (4:1), and UV absorbance of the solution was measured. Drug loading and encapsulation efficiency were calculated using eqs 1 and 2, respectively.

DOI: 10.1021/acsami.5b01786
ACS Appl. Mater. Interfaces 2015, 7, 9235−9246

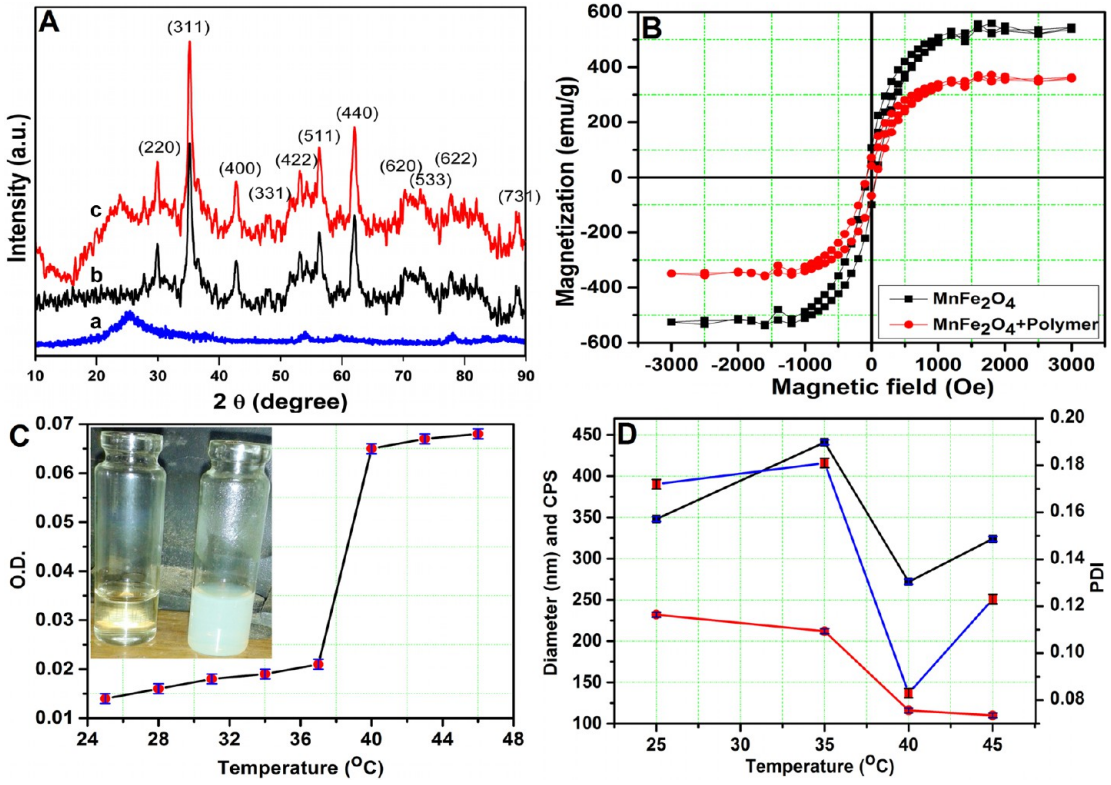

Figure 1. (A) XRD spectra of PNIPAm-*co*-GA (a), nonmodified (bare) $MnFe_2O_4$ nanoparticles (b), and poly-SPIONs (c). (B) Magnetic hysteresis loop of SPIONs and poly-SPIONs. (C) Cloud point measurement and (D) mean count rate (in kilo counts per second, kcps), poly dispersity index (PDI), and *z*-average diameter (nm) plotted as a function of temperature (°C) of poly-SPIONs. The inset shows a camera picture of poly-SPIONs below and above LCST.

$$\text{drug loading} = M_c/M_t \times 100 \quad (1)$$

$$\text{encapsulation efficiency} = M_c/M_0 \times 100 \quad (2)$$

where M_c is the amount of curcumin in the poly-SPIONs, M_0 is the total amount of curcumin, and M_t is the total amount of the poly-SPIONs. The concentration of the drug in the supernatant was determined by equating against a standard linear calibration plot of a concentration range of 2.0−25.0 mg L^{-1}.

2.10. In Vitro Drug Release Study. The cumulative drug release experiments were carried out at different conditions (temperature and pH) to evaluate the stimuli-response behavior of the poly-SPIONs. The release of curcumin from the drug loaded poly-SPIONs was carried out at physiological (7.4) and tumor extracellular pH (5.5) at three different temperatures (25, 37, and 40 °C). For each experiment, 110.0 μg of SPIONs loaded with 100 ppm curcumin (cur-SPIONs) was taken in 1.0 mL of water (pH = 7.4 or 5.5) and incubated in the above-mentioned temperatures. The amount of released drug was checked by a UV−visible spectrophotometer (420 nm) at different time intervals (30, 60, 90, 120, 150, 180, 210, 240, and 270 min). The percentage of released drug was calculated from a standard calibration curve of free drug solution.

2.11. Targeting of Drug Carrier to the Specific Site by Magnetic Capturing Test. To explore the target specific behavior of proposed magnetic nanoparticle, a magnetic capturing system was used which simulated the nature of real blood vessels in the body (Scheme S1, Supporting Information). It consisted of an injection pump, a 5.0 mL syringe, a silicon tube of 1.0 mm inner diameter, and a permanent magnet (max. flux density of 0.1 T). A 10.0 mL suspension of cur-SPIONs (2.0 μg mL^{-1}) was used for the test. First, the syringe was filled with the suspension and injected into one end of the tube. The magnet was fixed at the middle of tube, supposed to be the targeted site. The captured particles were accumulated at the middle of the tube, and the uncaptured samples were collected in a flask located outside of the magnetic system. The percentage of captured particles was determined by the weight difference using a UV−visible spectrophotometer.

2.12. In Vitro Cellular Uptake of Poly-SPIONs. The internalization of CMC−curcumin and cur-SPIONs into breast cancer cells (MCF7) was observed by fluorescence microscope imaging. For intracellular uptake studies, 10 μg mL^{-1} of the drug and/or nanoparticles was incubated with MCF7 cells for 1 and 4 h to determine the time dependent uptake of the drug and/or nanoparticles. After incubation, cells were fixed with 4% paraformaldehyde for 15 min, washed with PBS, and observed under a fluorescence microscope.

2.13. Cell Viability Study through the Methyl Thiazol Tetrazolium Bromide Assay. In vitro cytocompatibility of the poly-SPIONs with or without curcumin was investigated using a standard methyl thiazol tetrazolium bromide (MTT) assay on MCF7 cells. For this, MCF7 cells were seeded in 96-well plates in a growth medium consisting of Dulbecco's modified eagle media (DMEM) supplemented with 10% fetal bovine serum and 1% antibiotic solution and maintained at 37 °C in a humidified 5% CO_2 atmosphere. The cells were treated with various concentrations (0−30 μg mL^{-1}) of poly-SPIONs and cur-SPIONs and were cultured for another 24 h. After incubation, 20.0 μL of MTT was added to each well and the optical density was evaluated at 570 nm. Cell viability was calculated as follows:

$$\text{cell viability}(\%) = (A_{\text{sample}} - A_{\text{blank}}) \times 100\%/(A_{\text{control}} - A_{\text{blank}}) \quad (3)$$

where A_{sample} is the absorbance of a well with cells, MTT solution, and poly-SPIONs or cur-SPIONs; A_{blank} is the absorbance of a well with medium and MTT solution, without cells; A_{control} is the absorbance of a well with cells and MTT solution, without poly-SPIONs or cur-SPIONs. The data was expressed as the percentages of viable cells compared to the survival of a control group (untreated cells as controls of 100% viability).

DOI: 10.1021/acsami.5b01786
ACS Appl. Mater. Interfaces 2015, 7, 9235−9246

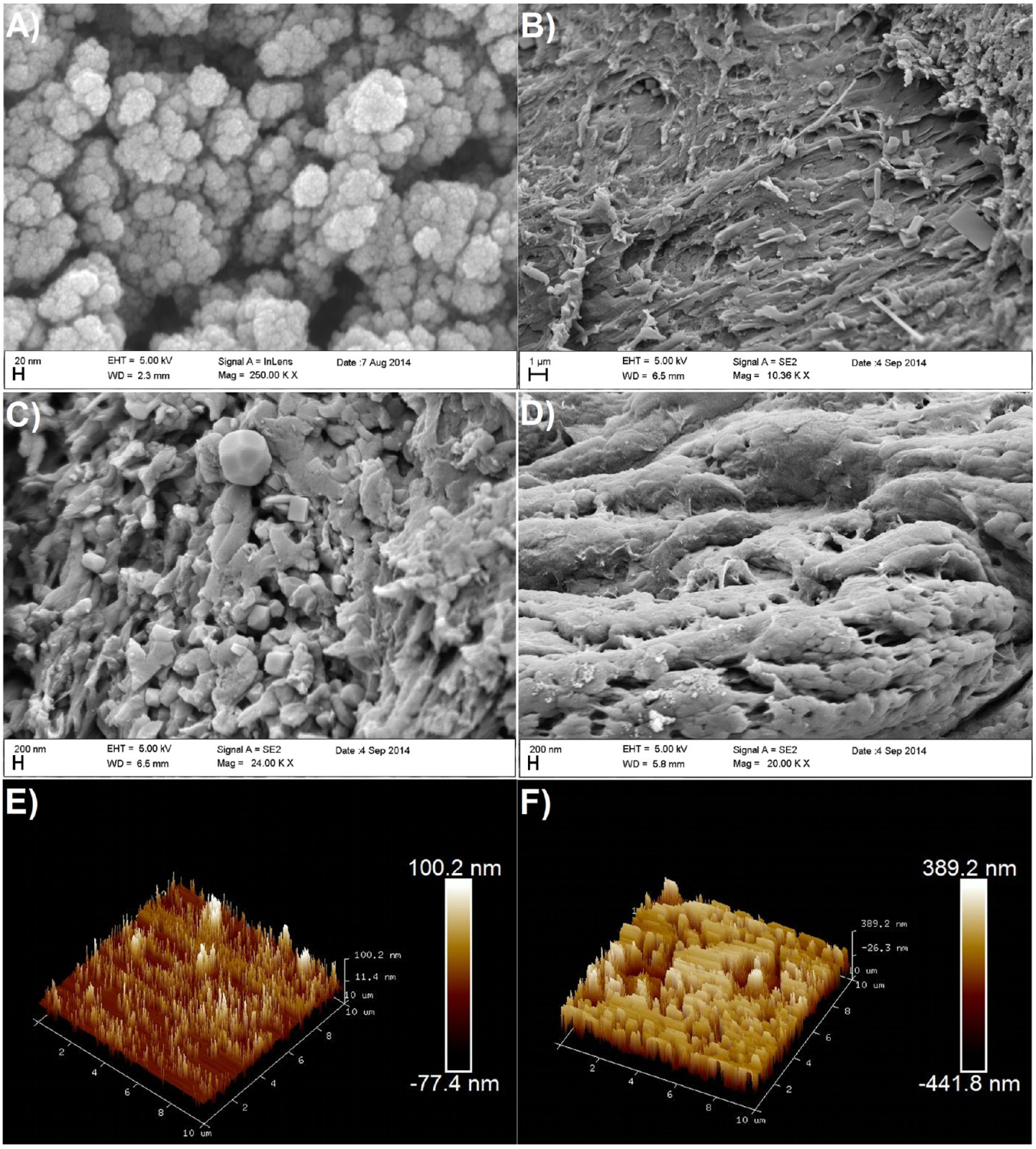

Figure 2. FE-SEM images of (A) nonmodified (bare), PNIPAm-*co*-GA (at low (B) and high resolutions (C)), and (D) PNIPAm-modified SPIONs. AFM images of (E) nonmodified (bare) and (F) PNIPAm-*co*-GA-modified SPIONs.

3. RESULTS AND DISCUSSION

3.1. X-ray Diffraction Studies. Figure 1A shows the XRD patterns of the PNIPAm (curve a), nonmodified (bare) $MnFe_2O_4$ nanoparticles (curve b), and poly-SPIONs (curve c). The strong diffraction peaks depicted in curve b at 29.65°, 34.9°, 42.4°, 46.4°, 52.6°, 56.1°, 61.5°, 69.8°, 72.7°, 73.7°, and 88.1° corresponds to (220), (311), (400), (331), (422), (511), (440), (620), (533), (622), and (731) planes, respectively (JCPDS file no. 73-1964). These diffraction peaks belong to the characteristic crystalline cubic structure (JCPDS file no. 73-1964) having space group *Fd*3*m* (227) of $MnFe_2O_4$. The XRD spectrum of PNIPAm-*co*-GA was also recorded as reference, which shows a broad peak at 25° (curve a). When the $MnFe_2O_4$ nanoparticles are coated with the polymer, a hump around 25° is observed, which confirms the successful coating of polymer on the SPIONs (curve c).

DOI: 10.1021/acsami.5b01786
ACS Appl. Mater. Interfaces 2015, 7, 9235−9246

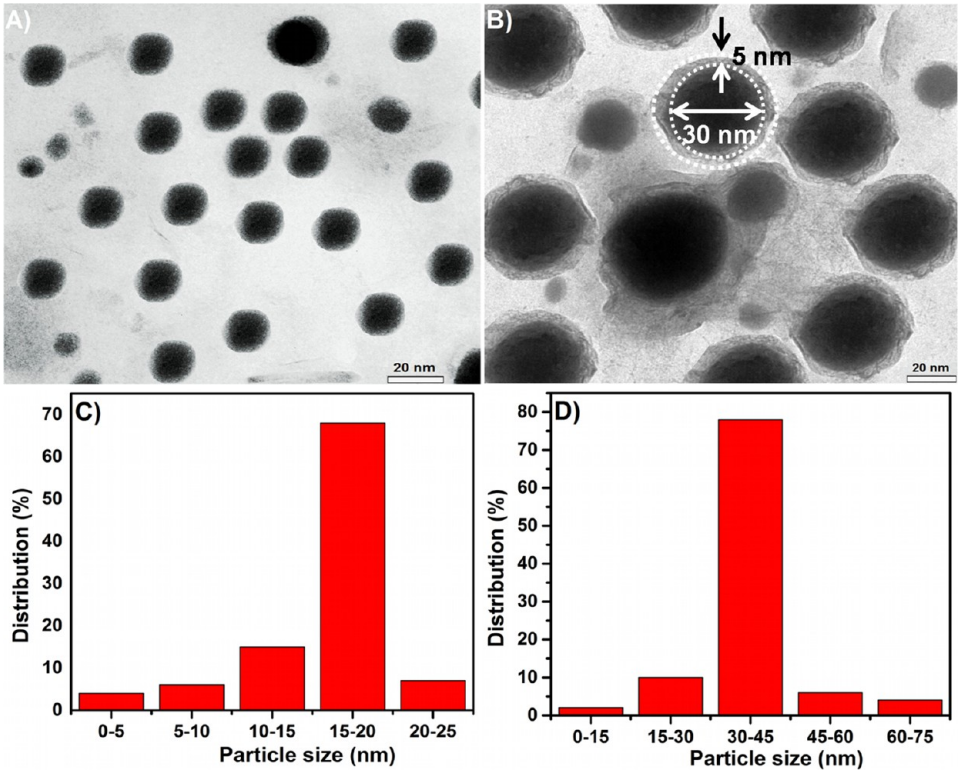

Figure 3. TEM (A and B) and particle size distribution images (C and D) of SPIONs and poly-SPIONs, respectively.

3.2. FE-SEM, AFM, and TEM Studies. Figure 2A shows the surface morphology and particulate structure of bare SPIONs by FE-SEM. Figure 2B,C shows the PNIPAm-*co*-GA modified SPIONs (poly-SPIONs) at low and high magnification. As shown in Figure 2B,C, SPIONs have a clear distribution of the spherical nanoparticle, but the SPIONs, modified with PNIPAm only, look like a fibrous surface in which nanoparticles are invisible (Figure 2D). This suggests the role of GA during polymerization, in which polymer prepared on SPIONs surface is more structured and well architected compared to the PNIPAm only. The surface topography of bare SPIONs and poly-SPIONs was again confirmed using an AFM. The AFM image of bare $MnFe_2O_4$ nanoparticles (Figure 2E) shows sharp particulate features/character whereas poly-SPIONs (Figure 2F) shows broad grain boundaries. The AFM results complement the FE-SEM observations.

The size, shape, and morphology of modified and unmodified nanoparticles were further confirmed by the TEM investigation. It was clearly shown in Figure 3A,C that the magnetic nanoparticles are well dispersed and are spherical in shape with a mean (±standard deviation) particle size 17 ± 2 nm. However, after polymer coating on the SPIONs, the particle size increased to 37 ± 3 nm (Figure 3D). Along with this, the presence of the inner magnetic core with an outer polymer layer with a thickness of 3−8 nm is clearly observed (Figure 3B). According to the literature, the most suitable particle size to penetrate the cancer cells is below 10 nm, but the particles of this size are rapidly cleared by the renal infiltration or excretion process. However, particles with a size of more than 50 nm are filtered out by the Kupffer cells of the liver,[28] treating them as a foreign substance, or sequestered by the reticuloendothelial system (RES) of the spleen and liver (>100 nm).[39] The nanoparticle size of <100 nm can easily evade RES, and therefore, the appropriate size of drug carriers and/or nanoparticles is in the range of 10−50 nm for magnetic hyperthermia applications.[19] Herein, the cur-SPIONs lie in this acceptable range and therefore can be used for drug delivery application.

3.3. Magnetic Property (VSM). For separation and hyperthermia applications, it is important that magnetic nanoparticles retain their favorable magnetic properties after modification with nonmagnetic polymers. Herein, the magnetic properties of both modified and nonmodified SPIONs were studied by VSM analysis. The room temperature magnetization curves of polymer modified and bare SPIONs are shown in Figure 1B. The saturation magnetization value of bare and poly-SPIONs was found to be 526.0 and 348.0 emu g^{-1}, respectively. The magnetization curve showed very small coercivity (41.29 Oe), which suggests the superparamagnetic nature of the prepared materials.[28] Superparamagnetism exhibited in the nanoparticles is due to their size effect (<50 nm) and mixed spinel structure, where each particle is a single magnetic domain and the energy barrier for their spin reversal is easily overcome by thermal vibrations.[19] In the mixed spinel structure, about 20% of the Mn^{2+} occupy octahedral (B) sites and the rest occupy tetrahedral (A) sites. However, the remaining tetrahedral and octahedral sites are occupied by Fe^{3+} metal ions.[28] This strong A−B interaction is also responsible for magnetic behavior of SPIONs. Figure S4, Supporting Information, illustrates that polymer modified SPIONs are active to the external magnetic field, where a magnet is able to manipulate the SPIONs within 20 s of time span. This important property of polymer coated SPIONs is in favor of targeted drug delivery of curcumin under the external magnetic field.

3.4. Determination of Lower Critical Solution Temperature of Polymer Modified SPIONs. Thermoresponsive polymers having a hydrophobic interaction with water

DOI: 10.1021/acsami.5b01786
ACS Appl. Mater. Interfaces 2015, 7, 9235−9246

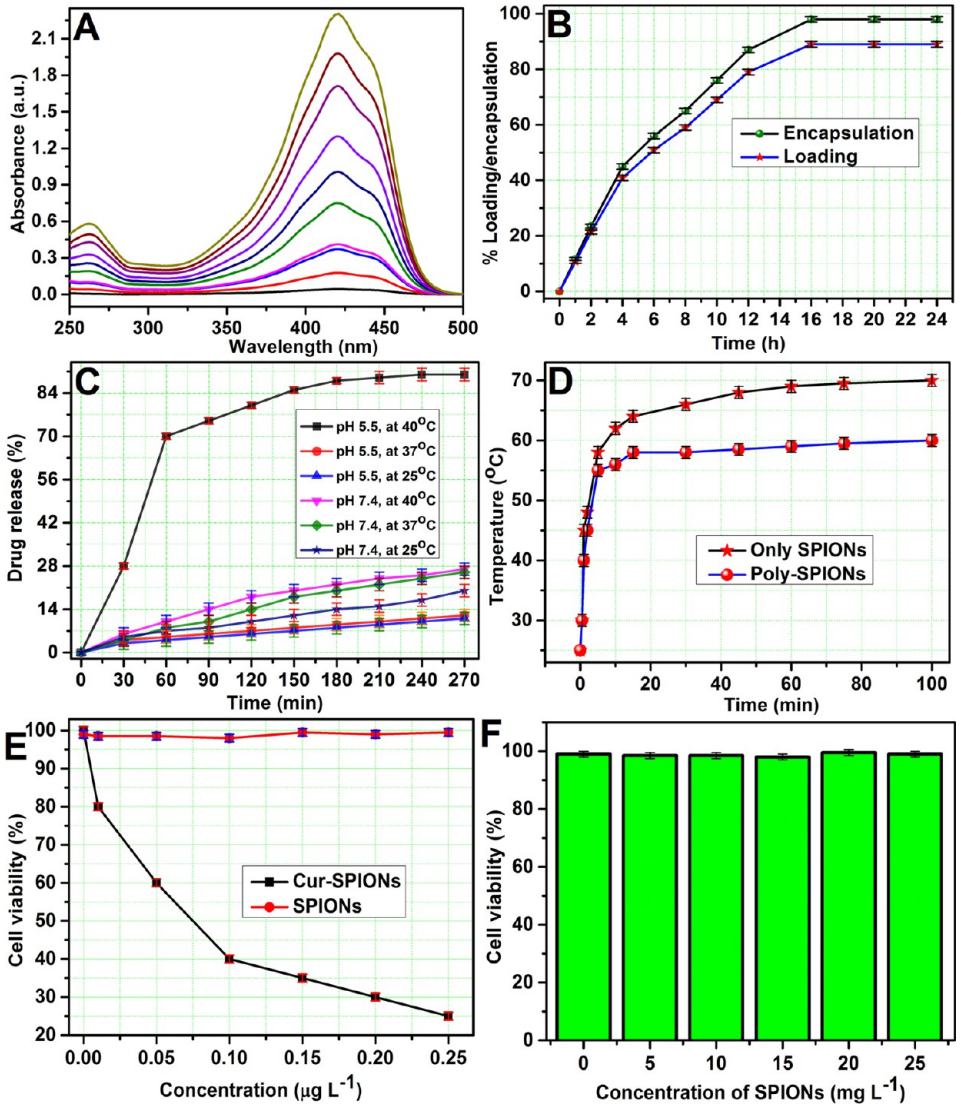

Figure 4. (A) UV−vis spectra of different concentrations of standard curcumin solutions in the range of 2.0−25.0 mg L^{-1}. (B) Plot of % encapsulation efficiency and loading capacity of poly-SPIONs. (C) Drug release profile for poly-SPIONs at different pH values (5.5 and 7.4) and temperatures (25, 37, and 40 °C). (D) Hyperthermia plot of SPIONs and poly-SPIONs showing an increase in temperature with a variation in time. (E) Cell viability study of poly-SPIONs (without curcumin) and curcumin loaded SPIONs on MCF7 cancer cells at low concentrations. (F) Cell viability study of MCF7 cancer cells in the presence of high concentrations of poly-SPIONs.

undergoes a phase transition from a swollen state at certain low temperatures to a collapsed state above that (high) temperature. Polymers, which become insoluble upon heating, have a so-called lower critical solution temperature (LCST). Below the LCST, the polymer is hydrophilic and becomes hydrophobic above this temperature, which can be visualized by the soluble and cloudy nature of the polymer at these temperatures (Figure 1C, inset). The LCST of polymer coated SPIONs with (PNIPAm-*co*-GA) and without GA (only PNIPAm) was estimated by heating the particles from 25 to 46 °C and studying the UV−visible spectrophotometer data at various temperatures (Figures 1C and S5, Supporting Information). From 25 °C to about 32 °C, the plot is almost horizontal undergoing the least absorption, indicating the copolymer to be hydrophilic in this temperature range. A sudden rise in absorption occurs at 32 °C in the polymer without GA (only PNIPAm) and at 40 °C in the case of PNIPAm-*co*-GA, which is supposed to be the LCST of the corresponding polymers. At this temperature, polymer becomes hydrophobic and expels water by dehydrating. Due to the shrinkage of copolymer volume, its porosity decreases and thus UV absorption increases for all temperatures above LCST. The variation in optical density and the increase of cloud point in the case of both the polymers confirms their thermoresponsive behavior. However, the role of GA is also confirmed here which causes an increase in the LCST value of PNIPAm.

3.5. Determination of Hydrodynamic Diameter of Polymer Modified SPIONs. The DLS measurement of the dispersed poly-SPIONs was performed at various temperatures and pH values to monitor their condition dependent change in hydrodynamic volume. As shown in Figure 1D, the mean count rate (in kilo counts per second (kcps)), poly dispersity index (PDI), and *z*-average diameter (nm) are plotted as a function of temperature (°C). As shown in the figure, the kcps, PDI, and average diameter of the particle decrease to their lowest values at the LCST, which suggests the thermoresponsive behavior of the polymer. A similar behavior was observed for the polymer modified SPIONs at pH 5.5. The variations of poly-SPIONs

DOI: 10.1021/acsami.5b01786
ACS Appl. Mater. Interfaces 2015, 7, 9235−9246

with both pH and temperature provide clear evidence for the formation of dual responsive polymer modified magnetic nanoparticles.

3.6. Drug Loading and Encapsulation Studies. The curcumin loading/encapsulation efficiencies were evaluated using a standard calibration curve obtained for a series of curcumin solutions (Figure S6, Supporting Information). The corresponding UV spectrum is given in Figure 4A. For drug loading, the poly-SPIONs were incubated with a CMC−curcumin solution, for different time intervals. After that, the nanoparticles were separated by an external magnet and the remaining curcumin present in the solution was extracted by ethyl acetate-propane-2-ol. The UV spectra were obtained for the extracted curcumin solutions and the corresponding drug loading was calculated (Figure S7, Supporting Information). As shown in the spectra, curcumin shows an intense peak at 425 nm, but after incubation with poly-SPIONs, the peak intensity continues to decrease, until 16 h of incubation. After that, the peak intensity remains constant, suggesting the saturated binding of drug to the poly-SPIONs.

Prior to studying the drug loading/encapsulation efficiencies of the poly-SPIONs, the amount of nanoparticle and concentration of the drug were optimized. It was found that 110 μg of poly-SPIONs with a curcumin concentration of 100 ppm gives a maximum of 45% encapsulation and 41% drug loading efficiency. Figure 4B shows the variation of drug loading/encapsulation in the poly-SPIONs with change in time, where drug loading/encapsulation efficiencies increase with increases in time. After 16 h of incubation, the highest loading capacity (89%) and encapsulation efficiency (98%) was observed. Afterward, drug loading was passive and almost smooth for hours later. The loading of curcumin into the poly-SPIONs is due to the noncovalent interaction between CMC and polymer functional groups present in the curcumin molecule. To further support the bonding between poly-SPIONs and curcumin, their UV spectra was also provided in the Supporting Information (Figure S8). First of all, the UV spectrum of curcumin was recorded, which gives a strong peak at 425 nm (curve 1). However, in the CMC−curcumin conjugate, the peak gets shifted and appears at 300 nm (curve 2). On the other hand, poly-SPIONs does not show any peaks in the UV spectra (curve 3), but when the poly-SPIONs get incubated with CMC−curcumin, it gives a peak at 350 nm, which suggests the bonding between curcumin and poly-SPIONs (curve 4). Due to the use of soluble CMC−curcumin conjugate and strong binding interaction between poly-SPIONs and curcumin in this work, the curcumin loading amount in the poly-SPIONs was found to be much higher compared to other polymeric drug carriers reported for curcumin. To support the high solubility of curcumin after loading, the camera picture of curcumin, CMC−curcumin, and cur-SPIONs in aqueous medium is given in Figure S9, Supporting Information. The cur-SPIONs (incubated for 16 h) were used for further drug release studies due to their high drug uptake.

3.7. In Vitro Drug Release Study. In vitro drug release from cur-SPIONs at different temperatures and pH values is shown in Figure 4C. The release was studied at three different temperatures: (1) below LCST (25 °C), (2) at body temperature (37 °C), and (3) at LCST (40 °C). Similarly, the two pH values selected here are 5.5 (pH value observed inside the tumor cells) and 7.4 (normal physiological pH). At normal pH, ∼6% drug release was observed at any temperature in the first 30 min, which increases to ∼20% after 150 min. This shows the specific delivery of drug carrier. However, in the same time span, at pH 5.5, the drug release is very slow when the temperature is below LCST, i.e., 25 and 37 °C. The drug release is at a maximum at pH 5.5 and temperature of 40 °C, where 28% release was obtained in the first 30 min and reached 85% in 150 min. The drug release profile confirms the dependence of release rate on variation in pH and temperature. Afterward, the rate of drug release was passive and smooth probably due to additional diffusion processes.

3.8. Magnetic Capture and Heat Generation Test (Hyperthermia). In general, it was shown that magnetic nanoparticles show a lower value of magnetization after modification with polymer. The lower value is related to the reduction in total magnetic content and an increase in nonmagnetic polymer. Herein, we adopted a very simple but effective test to explore the future in vivo application of poly-SPIONs. The experiment was divided in two sets. In the first one, magnetic heat-generation characteristics of SPIONs and poly-SPIONs were studied by dispersing the 25.0 μg of nanomaterials in 1 mL of water and subjecting them to an alternating magnetic field of 7.2 kA m^{-1} and frequency of 70 kHz for 1 h. In the second experiment, the approach of cur-SPIONs toward an external magnetic field was studied. Figure 4D shows the temperature variation with time of magnetic treatment. Initial temperatures were 25 °C for both observations. The temperature of the magnetic solution containing only SPIONs (nonmodified) increased to about 58 °C in 5 min, whereas polymer modified SPIONs caused a temperature increase of about 55 °C in the same time. Moreover, the temperature of the poly-SPIONs increased to 45 °C in ∼2 min, which is an effective and appropriate temperature for the localized hyperthermia treatment of cancer cells.[19]

The specific absorption rate (SAR) was also calculated to normalize the heating efficiency of these nanoparticles in W/g using the formula given below:[40]

$$\mathrm{SAR(W/g)} = C \times (\mathrm{d}T/\mathrm{d}t) \times (m_s/m_m)$$

where C is the specific heat capacity of suspension (=4.186 J g^{-1} $°C^{-1}$), $(\mathrm{d}T/\mathrm{d}t)$ is the slope of temperature versus time graph, m_s is the mass of suspension, and m_m is the mass of magnetic materials. The slope of the $\mathrm{d}T/\mathrm{d}t$ curve was measured by taking into account only the first 60 s. The SAR values for SPIONs and poly-SPIONs were calculated to be 112.18 and 84.38 W g^{-1}, respectively. Herein, it was found that the calculated SAR value of poly-SPIONs is lower than the SAR value of nonmodified SPIONs. However, it is sufficient enough for hyperthermia treatment.

Similarly, in the second set of experiments, the cur-SPIONs were targeted from one place to another using an external magnet (Scheme S1, Supporting Information). A camera photograph of the cur-SPIONs attracted by an external magnet is also presented (Figure S4, Supporting Information). Upon application of an external magnetic field to the bottle filled with the magnetic nanoparticle, the particles were deposited on the side of the bottle that was in close proximity to the magnet, and the dispersion was clear and transparent. Similarly, when the cur-SPIONs were injected at one end of the tube (assumed to be the blood vessel), they travel to the other end where the magnet is fixed and the remaining clear solution gets collected in the vial attached at the other end of the tube. Almost 99% of the nanoparticle gets accumulated around the magnet in 2 min by traveling the distance of 30 cm (Figure S4, Supporting

DOI: 10.1021/acsami.5b01786
ACS Appl. Mater. Interfaces 2015, 7, 9235−9246

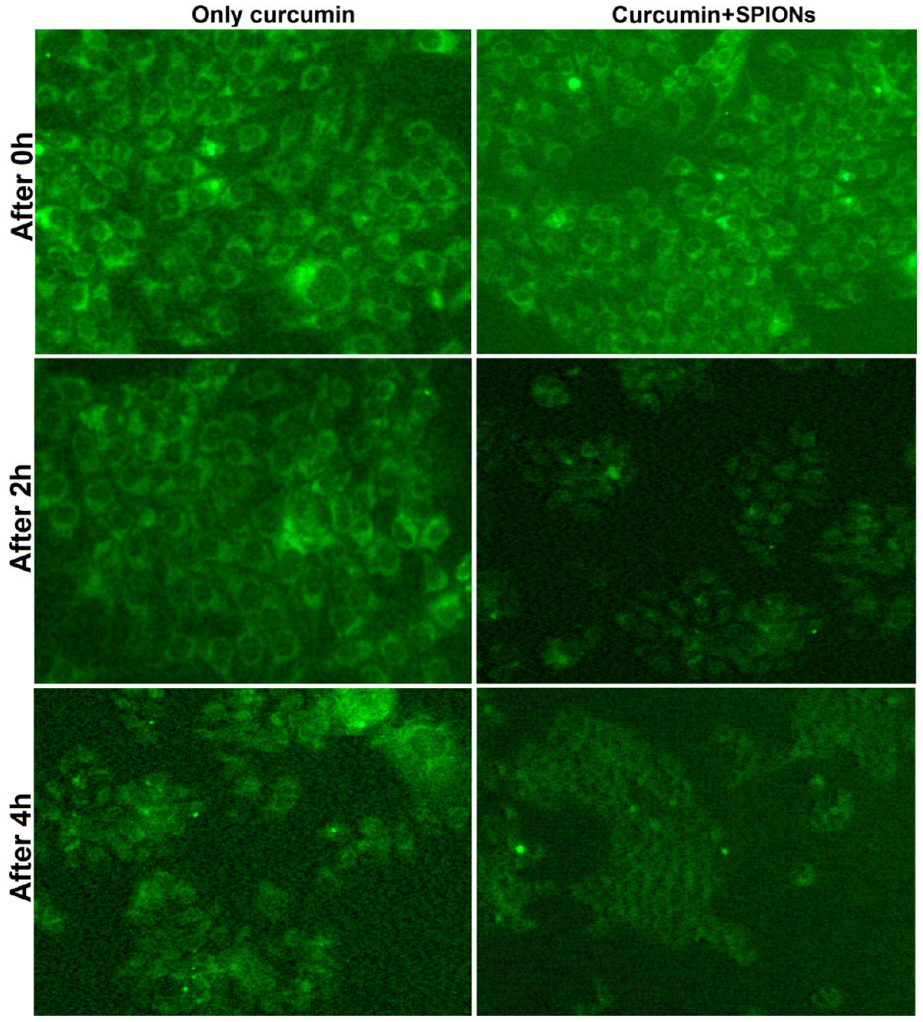

Figure 5. Confocal laser scanning fluorescence images of MCF7 cancer cells with only curcumin and curcumin loaded SPIONs at different incubation times.

Information). The experiment suggests the targeted delivery of curcumin at the required site.

3.9. Cellular Uptake Study by Fluorescence Imaging. The confocal laser scanning microscopic images for the curcumin only and cur-SPIONs were taken after excitation at 488 nm and presented in Figure 5. As portrayed in the images, initially, the cancer cells (MCF7) are healthy and clearly visualized, when drug or cur-SPIONs is just injected. However, after 2 h of incubation, the cells start dying in the presence of cur-SPIONs and remain healthy in the presence of curcumin only. After 4 h, almost all the cells become deformed in their shape and some changes are also visible in the curcumin only incubated cells. This may be due to poor solubility of curcumin inside the cancer cell, resulting in poor interaction and effect. However, in curcumin loaded SPIONs, more interaction occurs with cancer cells and as a consequence fast and effective results are obtained.

3.10. Cytocompatibility of Polymer Modified SPIONs (MTT Assay). Considering the high toxicity of acrylic monomers,[41] mainly for *N*-isopropylacrylamide, it is very important to examine the toxicity of polymers before employing them as a drug delivery system. In order to examine the acute toxicity of SPIONs, with and without drug, MCF7 cells were incubated for 12 h with poly-SPIONs in concentrations ranging from 0 to 0.25 μg L^{-1}. The cell viability, as determined with the MTT assay, demonstrated that cell lines incubated with poly-SPIONs are nontoxic at all tested concentrations, since the cell growth rates with poly-SPIONs are the same as that of the medium control. However, as shown in Figure 4E, the cell viability decreased remarkably against cur-SPIONs. Fewer than 25% of cells remain after incubation with 0.25 μg L^{-1} cur-SPIONs. However, at a very high concentration of 25 mg L^{-1}, none of the cells are affected in the presence of polymer modified SPIONs (without drug) (Figure 4F). The results demonstrate that synthesized poly-SPIONs do not show any cytotoxicity to both normal and cancer cells. The assay confirms the cytocompatibility as well as targeted drug delivery of curcumin. The results were well supported by an earlier reported study, in which Cooperstein and Canavan found that the NIPAm monomer in pure powdered form at 0.5 mg/mL was toxic to all tested cell types (endothelial, epithelial, fibroblast, and smooth muscle cells).[41] However, PNIPAm was not cytotoxic to the four cell types evaluated in the direct contact test. In addition, antibacterial properties of poly-SPIONs have been studied for *E. coli* and discussed in the Supporting Information (Sections S4 and S5, Figure S10).

DOI: 10.1021/acsami.5b01786
ACS Appl. Mater. Interfaces 2015, 7, 9235−9246

4. CONCLUSIONS

Dual responsive polymer modified water-soluble SPIONs attached with tagging agent (folic acid) were synthesized by a simple microwave technique. Curcumin, a hydrophobic anticancer drug, was used as a model compound to evaluate the characteristic features of poly-SPIONs. It was found that the cur-SPIONs are potentially capable of temperature and pH responsive targeted drug delivery of curcumin to cancer cells. The poly-SPIONs also show a very fast and efficient temperature increase when interacting with an external magnetic field. This may be due to the mixed spinel nature of SPIONs or their small size (15−20 nm). In the cell imaging, it was shown that poly-SPIONs were taken up specifically by MCF7 cancer cells and the drug was preferably released at pH 5.5 and temperature of 40 °C (LCST). Excellent efficacy for simultaneously targeting and destroying cancer cells was achieved. The loading capacity and encapsulation efficiency reached as high as 89% and 98%, respectively. From the MTT assay, it was also found that the poly-SPIONs are not harmful for cancer-cells but have a very good antibacterial property. From all the studies, it can be concluded that synthesized poly-SPIONs are excellent entities that may serve as carriers in cancer specific targeting, imaging, and therapeutic application in a single motif.

■ ASSOCIATED CONTENT

Supporting Information

Figure for magnetic capturing system (simulating a blood vessel), FT-IR spectra of CMC, CMC-SPIONs, cur-CMC, PNIPAm, PNIPAm-*co*-GA, and their discussions, camera images of poly-SPIONs in the presence of an external magnet, graph for cloud point measurement of PNIPAm by UV−visible spectroscopy, calibration curve for curcumin estimation by UV−visible spectroscopy, UV spectra for loading of curcumin into poly-SPIONs after different time intervals, UV spectra of curcumin, CMC−curcumin, poly-SPIONs, and cur-SPIONs, camera pictures of only curcumin, curcumin + CMC, and cur-SPIONs in aqueous medium, and antibacterial activity measurement by disc diffusion method and their growth kinetic study. This material is available free of charge via the Internet at http://pubs.acs.org.

■ AUTHOR INFORMATION

Corresponding Author

*E-mail: rshmmadhuri@gmail.com. Tel: +91 9471191640.

Notes

The authors declare no competing financial interest.

■ ACKNOWLEDGMENTS

Authors are thankful to Department of Science and Technology, Government of India for sanction of Fast Track Research Project for Young Scientists to Dr. Rashmi Madhuri (ref. No.: SB/FT/CS-155/2012) and Dr. Prashant K. Sharma (ref. No.: SR/FTP/PS-157/2011). Dr. Sharma (FRS/34/2012-2013/APH) and Dr. Madhuri (FRS/43/2013-2014/AC) are also thankful to Indian School of Mines, Dhanbad for grant of Major Research Project under Faculty Research Scheme. We are also thankful to Board of Research in Nuclear Sciences (BRNS), Department of Atomic Energy, Government of India for major research project.

■ REFERENCES

(1) Jong, W. H. D.; Borm, P. J. A. Drug Delivery and Nanoparticles: Applications and Hazards. *Int. J. Nanomed.* **2008**, *3*, 133−149.
(2) Kim, T. H.; Jiang, H. H.; Youn, Y. S.; Park, C. W.; Tak, K. K.; Lee, S.; Kim, H.; Jon, S.; Chen, X.; Lee, K. C. Preparation and Characterization of Water-Soluble Albumin-Bound Curcumin Nanoparticles with Improved Antitumor Activity. *Int. J. Pharm.* **2011**, *403*, 285−291.
(3) Wu, X.; Xu, J.; Huang, X.; Wen, C. Self-Microemulsifying Drug Delivery System Improves Curcumin Dissolution and Bioavailability. *Drug Dev. Ind. Pharm.* **2011**, *37*, 15−23.
(4) Dandawate, P. R.; Vyas, A.; Ahmad, A.; Banerjee, S.; Deshpande, J.; Swamy, K. V.; Jamadar, A.; Dumhe-Klaire, A. C.; Padhye, S.; Sarkar, F. H. Inclusion Complex of Novel Curcumin Analogue CDF and B-Cyclodextrin (1:2) and Its Enhanced in Vivo Anticancer Activity Against Pancreatic Cancer. *Pharm. Res.* **2012**, *29*, 1775−1786.
(5) Harada, T.; Pham, D. T.; Leung, M. H.; Ngo, H. T.; Lincoln, S. F.; Easton, C. J.; Kee, T. W. Cooperative Binding and Stabilization of the Medicinal Pigment Curcumin by Diamide Linked Γ-Cyclodextrin Dimers: A Spectroscopic Characterization. *J. Phys. Chem. B* **2011**, *115*, 1268−1274.
(6) Yallapu, M. M.; Jaggi, M.; Chauhan, S. C. Poly(B-Cyclodextrin)/Curcumin Self-Assembly: A Novel Approach to Improve Curcumin Delivery and Its Therapeutic Efficacy in Prostate Cancer Cells. *Macromol. Biosci.* **2010**, *10*, 1141−1151.
(7) Hegge, A. B.; Schuller, R. B.; Kristensen, S.; Tonnesen, H. H. In Vitro Release of Curcumin from Vehicles Containing Alginate and Cyclodextrin. Studies of Curcumin and Curcuminoides. *Pharmazie* **2008**, *63*, 585−592.
(8) Dey, S.; Sreenivasan, K. Conjugation of Curcumin onto Alginate Enhances Aqueous Solubility and Stability of Curcumin. *Carbohydr. Polym.* **2014**, *99*, 499−507.
(9) Drakalska, E.; Momekova, D.; Manolova, Y.; Budurova, D.; Momekov, G.; Genova, M.; Antonov, L.; Lambov, N.; Rangelov, S. Hybrid Liposomal Pegylated Calix[4]Arene Systems as Drug Delivery Platforms for Curcumin. *Int. J. Pharm.* **2014**, *472*, 165−174.
(10) Baruah, B.; Saikia, P. M.; Dutta, R. K. Binding and Stabilization of Curcumin by Mixed Chitosan−Surfactant Systems: A Spectroscopic Study. *J. Photochem. Photobiol., B* **2012**, *245*, 18−27.
(11) Berginc, K.; Suljakovic, S.; Skalko-Basnet, N.; Kristl, A. Mucoadhesive Liposomes as New Formulation for Vaginal Delivery of Curcumin. *Eur. J. Pharm. Biopharm.* **2014**, *87*, 40−46.
(12) Li, C.; Zhang, Y.; Su, T.; Feng, L.; Long, Y.; Chen, Z. Silica-Coated Flexible Liposomes as a Nanohybrid Delivery System for Enhanced Oral Bioavailability of Curcumin. *Int. J. Nanomed.* **2012**, *7*, 5995−6002.
(13) Altunbas, A.; Lee, S. J.; Rajasekaran, S. A.; Schneider, J. P.; Pochan, D. J. Encapsulation of Curcumin in Self-Assembling Peptide Hydrogels as Injectable Drug Delivery Vehicles. *Biomaterials* **2011**, *32*, 5906−5914.
(14) Zhongfa, L.; Chiu, M.; Wang, J.; Chen, W.; Yen, W.; Fan Havard, P.; Yee, L. D.; Chan, K. K. Enhancement of Curcumin Oral Absorption and Pharmacokinetics of Curcuminoids and Curcumin Metabolites in Mice. *Cancer Chemother. Pharmacol.* **2012**, *69*, 679−689.
(15) Gao, Y.; Li, Z.; Sun, M.; Li, H.; Guo, C.; Cui, J.; Li, A.; Cao, F.; Xi, Y.; Lou, H.; Zhai, G. Preparation, Characterization, Pharmacokinetics, and Tissue Distribution of Curcuma Nanosuspension with TPGS as Stabilizer. *Drug Dev. Ind. Pharm.* **2010**, *36*, 1225−1234.
(16) Gota, V. S.; Maru, G. B.; Soni, T. G.; Gandhi, T. R.; Kochar, N.; Agarwal, M. G. Safety and Pharmacokinetics of a Solid Lipid Curcumin Particle Formulation in Osteosarcoma Patients and Healthy Volunteers. *J. Agric. Food Chem.* **2010**, *58*, 2095−2099.
(17) Khalil, N. M.; do Nascimento, T. C.; Casa, D. M.; Dalmolin, L. F.; de Mattos, A. C.; Hoss, I.; Romano, M. A.; Mainardes, R. M. Pharmacokinetics of Curcumin-Loaded PLGA and PLGA−PEG Blend Nanoparticles after Oral Administration in Rats. *Colloids Surf., B* **2013**, *101*, 353−360.

DOI: 10.1021/acsami.5b01786
ACS Appl. Mater. Interfaces 2015, 7, 9235−9246

(18) Chomoucka, J.; Drbohlavova, J.; Huska, D.; Adam, V.; Kizek, R.; Hubalek, J. Magnetic Nanoparticles and Targeted Drug Delivering. *Pharmacol. Res.* **2010**, *62*, 144−149.
(19) Kim, D.-H.; Nikles, D. E.; Brazel, C. S. Synthesis and Characterization of Multifunctional Chitosan-$MnFe_2O_4$ Nanoparticles for Magnetic Hyperthermia and Drug Delivery. *Materials* **2010**, *3*, 4051−4065.
(20) Shah, S. A.; Hashmi, M. U.; Alam, S.; Shamim, A. Effect of Aligning Magnetic Field on the Magnetic and Calorimetric Properties of Ferrimagnetic Bioactive Glass Ceramics for the Hyperthermia Treatment of Cancer. *Mater. Sci. Eng., C* **2011**, *3*, 1010−1016.
(21) Cheng, K. K.; Chan, P. S.; Fan, S.; Kwan, S. M.; Yeung, K. L.; Wang, Y.-X. J.; Chow, A. H. L.; Wu, E. X.; Baum, L. Curcumin-Conjugated Magnetic Nanoparticles for Detecting Amyloid Plaques in Alzheimer's Disease Mice Using Magnetic Resonance Imaging (MRI). *Biomaterials* **2015**, *44*, 155−172.
(22) Sundar, S.; Mariappan, R.; Piraman, S. Synthesis and Characterization of Amine Modified Magnetite Nanoparticles as Carriers of Curcumin-Anticancer Drug. *Powder Technol.* **2014**, *266*, 321−328.
(23) Tran, L. D.; Hoang, N. M. T.; Mai, T. T.; Tran, H. V.; Nguyen, N. T.; Tran, T. D.; Do, M. H.; Nguyen, Q. T.; Pham, D. G.; Ha, T. P.; Le, H. V.; Nguyen, P. X. Nanosized Magnetofluorescent Fe_3O_4−Curcumin Conjugate for Multimodal Monitoring and Drug Targeting. *Colloids Surf., A* **2010**, *371*, 104−112.
(24) Konwarh, R.; Saikia, J. P.; Karak, N.; Konwar, B. K. 'Poly(ethylene glycol)-Magnetic Nanoparticles-Curcumin' Trio: Directed Morphogenesis and Synergistic Free-Radical Scavenging. *Colloids Surf., B* **2010**, *81*, 578−586.
(25) Fundueanu, G.; Constantin, M.; Oanea, I.; Harabagiu, V.; Ascenzi, P.; Simionescu, B. C. Prediction of the Appropriate Size of Drug Molecules That Could be Released by a Pulsatile Mechanism from pH/Thermoresponsive Microspheres Obtained from Preformed Polymers. *Acta Biomater.* **2012**, *8*, 1281−1289.
(26) Liu, Y.; Wang, W.; Yang, J.; Zhou, C.; Sun, J. pH-Sensitive Polymeric Micelles Triggered Drug Release for Extracellular and Intracellular Drug Targeting Delivery. *Asian J. Pharm. Sci.* **2013**, *8*, 159−167.
(27) Roy, D.; Brooks, W. L. A.; Sumerlin, B. S. New Directions in Thermo Responsive Polymers. *Chem. Soc. Rev.* **2013**, *42*, 7214−7243.
(28) Shah, S. A.; Asdi, M. H.; Hashmi, M. U.; Umar, M. F.; Awan, S.-U. Thermo-Responsive Copolymer Coated $MnFe_2O_4$ Magnetic Nanoparticles for Hyperthermia Therapy and Controlled Drug Delivery. *Mater. Chem. Phys.* **2012**, *137*, 365−371.
(29) Saitoh, T.; Asano, K.; Hiraide, M. Removal of Phenols in Water Using Chitosan-Conjugated Thermo-Responsive Polymers. *J. Hazard. Mater.* **2011**, *185*, 1369−1373.
(30) Papagiannopoulos, A.; Zhao, J.; Zhang, G.; Pispas, S.; Radulescu, A. Thermoresponsive Aggregation of PS−PNIPAM−PS Triblock Copolymer: A Combined Study of Light Scattering and Small Angle Neutron Scattering. *Eur. Polym. J.* **2014**, *56*, 59−68.
(31) Dhanya, S.; Bahadur, D.; Kundu, G. C.; Srivastava, R. Maleic Acid Incorporated Poly-(*N*-isopropylacrylamide) Polymer Nanogels for Dual-Responsive Delivery of Doxorubicin Hydrochloride. *Eur. Polym. J.* **2013**, *49*, 22−32.
(32) Wakamatsu, H.; Yamamoto, K.; Nakao, A.; Aoyagi, T. Preparation and Characterization of Temperature-Responsive Magnetite Nanoparticles Conjugated with *N*-Isopropylacrylamide-Based Functional Copolymer. *J. Magn. Magn. Mater.* **2006**, *302*, 327−333.
(33) Saeed, A.; Georget, D. M. R.; Mayes, A. G. Solution Thermal Properties of a Family of Thermo-Responsive *N*-Isopropylacrylamide-co-*N*-hydroxymethylacrylamide Copolymers − Aspects Intrinsic to the Polymers. *React. Funct. Polym.* **2012**, *72*, 77−82.
(34) Sahoo, B.; Devi, K. S. P.; Banerjee, R.; Maiti, T. K.; Pramanik, P.; Dhara, D. Thermal and pH Responsive Polymer-Tethered Multifunctional Magnetic Nanoparticle for Targeted Delivery of Anticancer Drug. *ACS Appl. Mater. Interfaces* **2013**, *5*, 3884−3893.
(35) Yadavalli, T.; Ramasamy, S.; Chandrasekaran, G.; Michael, I.; Therese, H. A.; Chennakesavulu, R. Dual Responsive PNIPAM-Chitosan Targeted Magnetic Nanopolymer for Targeted Drug Delivery. *J. Magn. Magn. Mater.* **2015**, *380*, 315−320.
(36) Aslibeiki, B.; Kameli, P. Magnetic Properties of $MnFe_2O_4$ Nano-Aggregates Dispersed in Paraffin Wax. *J. Magn. Magn. Mater.* **2015**, *385*, 308−312.
(37) Patra, S.; Roy, E.; Madhuri, R.; Sharma, P. K. An Imprinted Ag@CdS Core Shell Nanoparticle Based Optical-Electrochemical Dual Probe for Trace Level Recognition of Ferritin. *Biosens. Bioelectron.* **2015**, *63*, 301−310.
(38) Patra, S.; Roy, E.; Madhuri, R.; Sharma, P. K. Imprinted ZnO Nanostructure-Based Electrochemical Sensing of Calcitonin: A Clinical Marker for Medullary Thyroid Carcinoma. *Anal. Chim. Acta* **2015**, *853*, 271−284.
(39) Shubayev, V. I.; Pisanic, T. R., II; Jin, S. Magnetic Nanoparticles for Theragnostics. *Adv. Drug Delivery Rev.* **2009**, *61*, 467−477.
(40) Prasad, N. K.; Rathinasamy, K.; Panda, D.; Bahadur, D. Mechanism of Cell Death Induced by Magnetic Hyperthermia with Nanoparticles of γ-$Mn_xFe_{2-x}O_3$ Synthesized by a Single Step Process. *J. Mater. Chem.* **2007**, *17*, 5042−5051.
(41) Cooperstein, M. A.; Canavan, H. E. Assessment of Cytotoxicity of (*N*-Isopropyl Acrylamide) and Poly(*N*-isopropyl Acrylamide)-Coated Surfaces. *Biointerphases* **2013**, *8*, 19.

DOI: 10.1021/acsami.5b01786
ACS Appl. Mater. Interfaces 2015, 7, 9235−9246